Effects of Oxygen on the Growth Characteristics of Carbon Nanotubes on Conductive Substrates

by

Ryan K. Bonaparte

Submitted to the Department of Materials Science and Engineering in partial fulfillment of the Requirements for the Degree of

BACHELOR OF SCIENCE

at the

MASSACHUSETTS INSTITUTE OF TECHNOLOGY

June 2009

Signature of Author _____
Department of Materials Science and Engineering
May 13, 2009

Certified by _____
Carl V. Thompson
Stavros Salapatas Professor
Thesis Supervisor, Department of Materials Science and Engineering

Accepted by _____
Professor Lionel C. Kimerling
Chair, Undergraduate Committee
Department of Materials Science and Engineering

Effects of Oxygen on the Growth Characteristics of

Carbon Nanotubes on Conductive Substrates

by

Ryan K. Bonaparte

Submitted to the Department of Materials Science and Engineering on May 13th, 2009, in partial fulfillment of the requirements for the degree of Bachelor of Science in Materials Science and Engineering

Abstract

The effects of oxygen on Fe-catalyzed carbon nanotube (CNT) growth on Ta substrates was studied. CNTs were grown on Fe thin-film catalysts deposited on silicon substrates via exposure to C_2H_4 in a thermal chemical vapor deposition (CVD) furnace. Heating for CVD growth causes the Fe film to dewet to form catalyst particles. During CVD, the sample was exposed to gas mixtures of Ar, Ar/O_2, H_2, and C_2H_4. Experiments were performed with varying amounts of oxygen from mixing of the Ar and Ar/O_2 carrier gas, as well as pre-annealing samples in oxygen or hydrogen-rich environments. Samples were characterized via scanning electron microscopy (SEM) and atomic force microscopy (AFM). It was found that when an optimum amount of oxygen was introduced, taller CNT carpets were observed. Pre-annealing samples in an oxygen-rich environment shows additional benefits in carpet growth. In contrast, pre-annealing in a hydrogen-rich environment counteracts the benefits of introducing oxygen during the growth phase. Coarsening of the catalyst particles was suspected as a reason for the difference in growth patterns, and pre-annealed sample morphologies were characterized without C_2H_4 flow. AFM scans show apparent coarsening in samples exposed to hydrogen-rich environments, and reduced coarsening in the samples exposed to oxygen-rich environments.

Thesis Supervisor: Carl V. Thompson

Title: Stavros Salapatas Professor, Department of Materials Science and Engineering

Table of Contents

List of Figures

List of Tables

Motivation

Of the many properties of carbon nanotubes (CNTs), the electronic behavior is of particular interest to this project. With conductivities surpassing that of copper, CNTs have the potential of replacing copper in many of the electronic devices that rely on the electrical conductance of copper. In particular, the microprocessor industry relies heavily on copper to serve as interconnects between successive layers throughout integrated circuits (IC). Copper has shown to be very useful in this application, with it's high conductivity it is a material used throughout the industry, though it is beginning to reach its physical limits as the ICs are developed into smaller devices. Copper begins to break down from the relatively large currents flown through the interconnects, which causes device malfunction. As there is roughly 2-3 km of copper material within a standard microprocessor, any breaks in the sections of wiring would disrupt processing functions. This has led to potentially serious difficulties in the further development of smaller microprocessors. CNTs are seen as a possible replacement material as they have been shown to possess similar properties as copper, but do not succumb to the same failings.

Before CNTs can be incorporated into these devices, there are a few technical hurdles that must be overcome. First, ICs are manufactured at relatively low temperatures to control the level of diffusion of dopants and other materials throughout the processing steps. To include CNTs in these processes, they must be able to be grown at similar temperatures. Many researchers have been unable to reach this goal, which currently stands at unknown. Secondly, the CNTs must be grown on a conductive substrate. Most research performed to date has shown the ability to grow fairly large CNTs, on the order of millimeters, but only on insulating substrates. (Futaba, Hata, & Iijima, 2006) Additionally, the CNTs must be grown in predictable

directions and locations. IC applications require nanometer precision for the placement of interconnects and any replacement technology must be able to replicate this fact. Finally, CNTs must be able to be grown using methods that are easily replicated, as the extremely high output of the semiconductor industry requires any new technologies to be easily adapted into the streamlined process.

Background

The growth characteristics of carbon nanotubes are of great interest, as the potential incorporation of carbon nanotubes in devices requires the controlled growth in defined areas.

Carbon Structures

Carbon, a ubiquitous element, can take the form of many structures. With structures ranging in use from graphite, which is often used in writing utensils, to diamond, an extremely hard material often incorporated in tools for machining. There are various other forms possible, some of which are shown below.

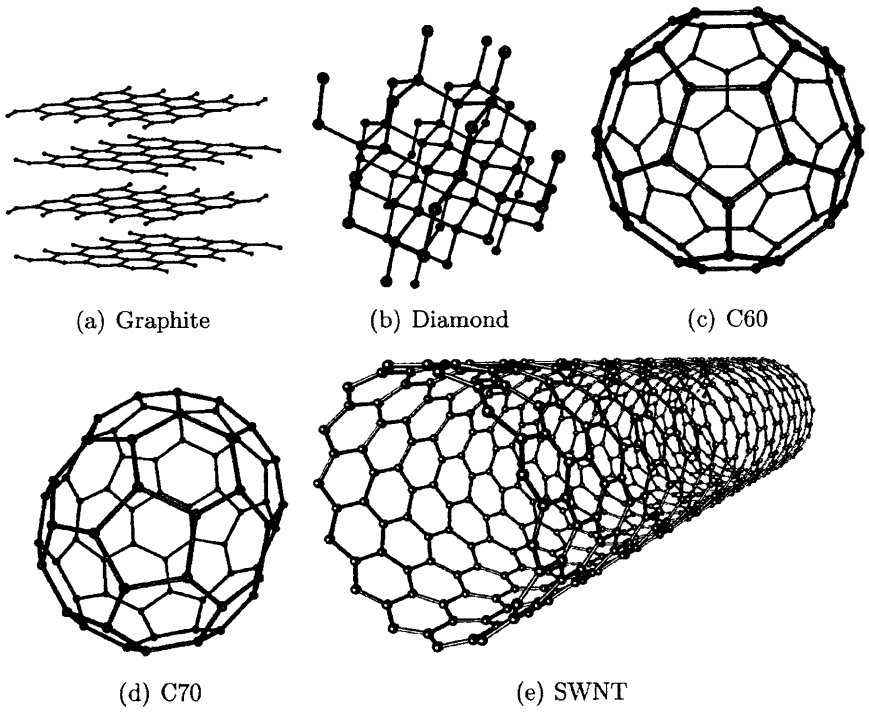

Figure 1. Various structures of Carbon.
(Seita, 2007)

Structure of Carbon Nanotubes

Carbon nanotubes are composed entirely of carbon with a structure similar to that of a sheet of graphene. Graphene is found as hexagonal rings in a single layer sheet, but can form a tube like shape, as if the sheet were rolled up, which is the structure held by CNT. Though this is not how carbon nanotubes are formed, it serves as a good visual representation of their physical structure.

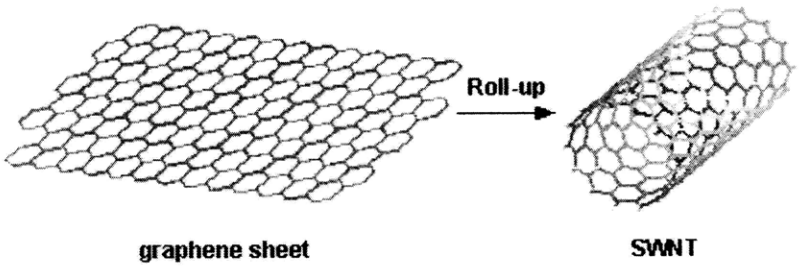

Figure 2. Representation of structure of CNT.
(Odom, Huang, Kim, & Lieber, 2000)

Types

There are two particular types of CNT that are of interest: Single Wall (SWCNT) and Multi-Wall (MWCNT) Carbon Nanotubes. The difference between these two types are as the name suggests; SWCNT are composed of a single layer of graphene, while MWCNT consist of multiple layers. These variations can lead to different sizes, dimensions, as well as properties.

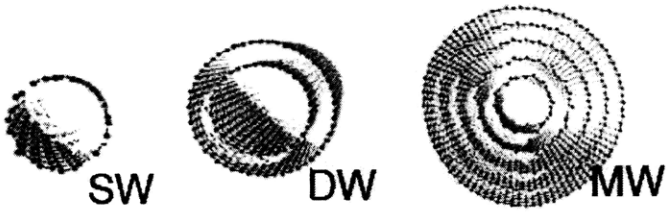

Figure 3. Cross sectional view of SWNT, Dual-wall CNT (DWNT), and MWNT.
(Seita, 2007)

Growth Mechanisms

The growth mechanisms for CNTs are not fully understood, but there are theories that present hypotheses supported by observed results. The two types of growth presented in the literature are tip-growth and base-growth. Both mechanisms operate by the introduction a carbon source into an environment in which it is able to disassociate and proceed to a catalyst.

In tip-growth, the carbon is thought to move along the surface of the catalyst towards the substrate. When near the bottom of the catalyst particle, the carbon forms a tube-like structure and pushes the catalyst away from the surface as it grows.

In base-growth, the opposite occurs. The carbon travels along the surface of the catalyst towards the top of the particle. The carbon then forms the tube on top of the catalyst and leaves the catalyst on the surface. Hata and Iijima (Hata, Futaba, Mizuno, Namai, Yumura, & Iijima, 2004) have proven this growth is possible by removing CNTs from a surface, leaving only the bottom portion and catalyst present, from which regrowth was possible.

Chirality

One of the most important structural properties of a CNT is the chirality, as many of the other properties, such as electrical activity, are heavily reliant on the chirality and diameter. Chirality is defined by the number of twists a tube experiences in a single turn of its diameter. These twists can be visualized a vector, termed the chiral vector, c, which is depicted in **Figure 4**.

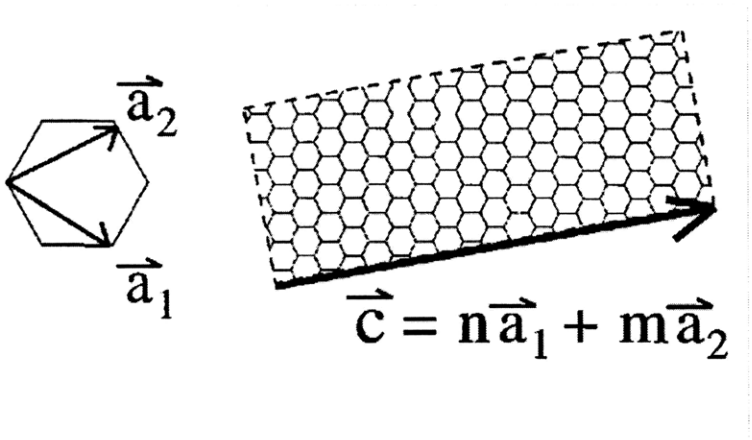

Figure 4. Chiral Vector.
The vector, c, that describes the chirality in an "unraveled" strip of graphene.
(Dresselhaus, Dresselhaus, & Avouris, 2001)

The chiral angle is an important component in defining the charility, as it is the angle at which a chiral vector runs along the length of a CNT. The chiral angle is shown in **Figure 5** can be summarized by **Equation 1**,

Equation 1

$$\text{Chiral Angle} = \tan^{-1}(\sqrt{3}n/(2m + n))$$

where n and m are integer components of a chiral vector defined as (n,m). The chiral angle is measured along the surface of the tube and leads to three distinct configurations: zig-zag (either n or m = 0), armchair (n=m), and chiral (other n,m combinations).

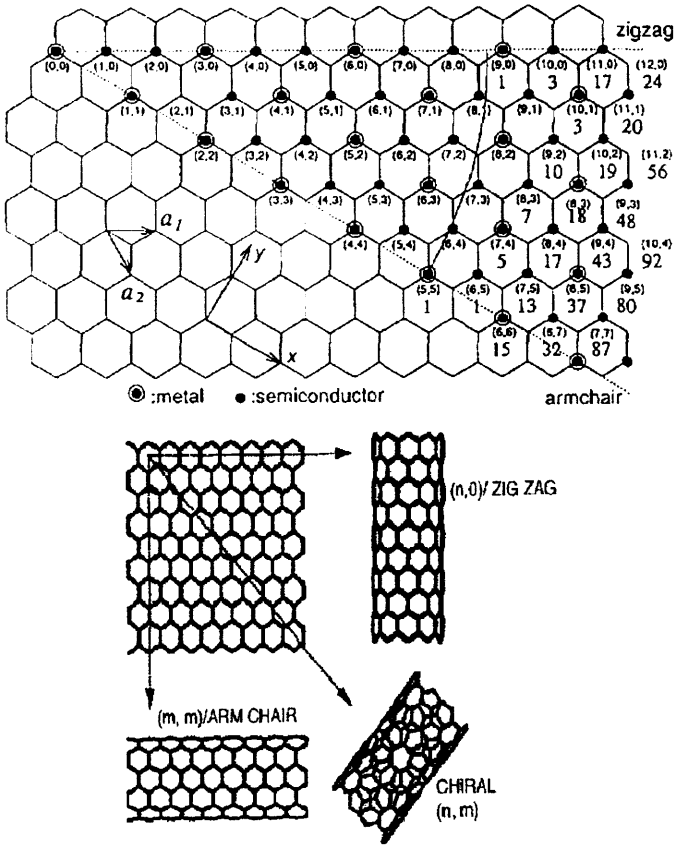

Figure 5. Expanded View of Chirality.
(Seita, 2007)

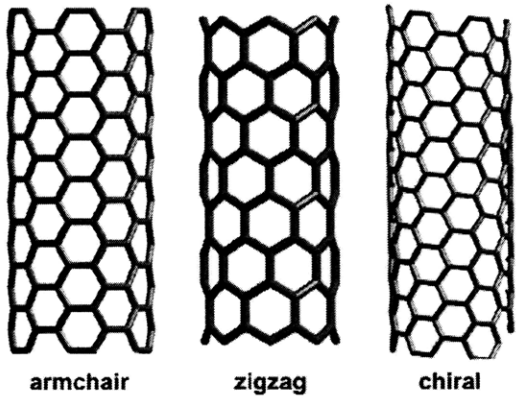

Figure 6. Different possible twists of CNT.
http://coecs.ou.edu/Brian.P.Grady/nanotube.html

Properties of Carbon Nanotubes

The properties of CNTs are of great interest, as the mechanical, chemical, and electrical properties all exhibit extraordinary behavior. Due to the delocalization of electrons in the carbon π-bonds, CNTs can be extremely conductive materials. Below is a table containing a tabulation of many of the standard properties. Many of these properties are estimated/theoretical maximums and are strongly dependent on the processing methods used to grow the CNTs.

Table 1. Extended Properties of CNT.
(Seita, 2007)

Equilibrium Structure	
Average Diameter of SWNTs:	$1.2 - 1.4nm$
Carbon Bond Length	$1.42\mathring{A}$
C-C Tight Bonding Overlap Energy	$\sim 2.5eV$
Lattice Constant	$17\mathring{A}$
Lattice Parameter	
(10, 10) Armchair	$16.78\mathring{A}$
(17, 0) Zigzag	$16.52\mathring{A}$
(12, 6) Chiral	$16.52\mathring{A}$
Density	
(10, 10) Armchair	$1.33g/cm^3$
(17, 0) Zigzag	$1.34g/cm^3$
(12, 6) Chiral	$1.40g/cm^3$
Interlayer Spacing	
(10, 10) Armchair	$3.38\mathring{A}$
(17, 0) Zigzag	$3.41\mathring{A}$
(12, 6) Chiral	$3.39\mathring{A}$
Optical Properties	
Fundamental Gap of a metallic tube:	$0eV$
Fundamental Gap of a semiconducting tube:	$\sim 0.5eV$
Electrical Transport	
Conductance Quantization	$n \times (12.9k\Omega)^{-1}$
Resistivity	$10^{-4}\Omega \cdot cm$
Maximum Current Density	$10^{13}A/m^2$
Thermal Transport	
Thermal Conductivity(RT)	$\sim 2000W/m \cdot K$
Phonon Mean Free Path	$\sim 100nm$
Relaxation Time	$\sim 10^{-11}s$
Elastic Behavior	
Young's Modulus (SWNT)	$\sim 1TPa$
Young's Modulus (MWNT)	$1.28TPa$
Maximum Tensile Strength	$\sim 30GPa$

Growth Techniques

There are various methods for growing CNTs: Arc-Discharge, Plasma Enhanced Chemical Vapor Deposition (PECVD) and Thermal Chemical Vapor Deposition (CVD) are among the most common. For the purposes of this research Thermal CVD was used.

Thermal CVD

The process for growth involved the following setup. A three-zone furnace is used to heat the gasses leading to the disassociation of the carbon source into individual carbon atoms for deposition on to a substrate. The substrate must have a catalyst on the surface in order to promote the growth of CNTs as opposed to other structures, amorphous carbon, or nothing at all. The gases flow into a quartz tube located within the furnace with a waiting preloaded substrate outside of the furnace. There are various mixtures of gasses and temperature profiles that can produce CNT as well as other carbon formations.

By using a three-zone furnace the temperature of the substrate can be set at a different temperature than the incoming gasses are exposed to "up stream." This is a critical component, as the experiments must be proven to work in similar conditions to those that are found in the semiconductor industry. Once the furnace reaches an appropriate temperature, the sample is loaded into the furnace in a process known as "fast-heating." A picture of the furnace setup and a schematic of fast-heat approach are depicted below.

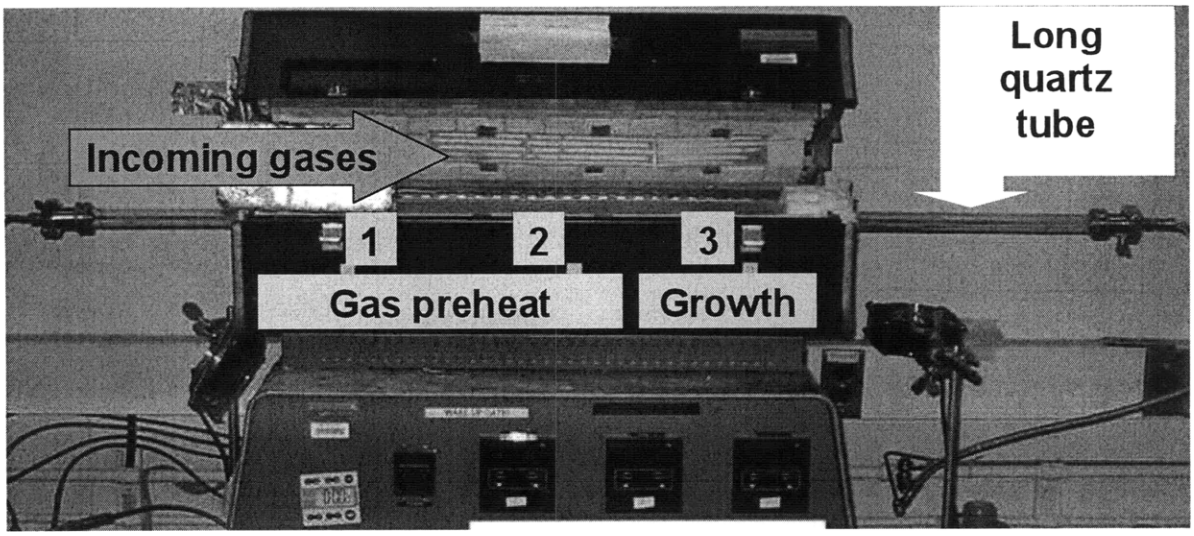

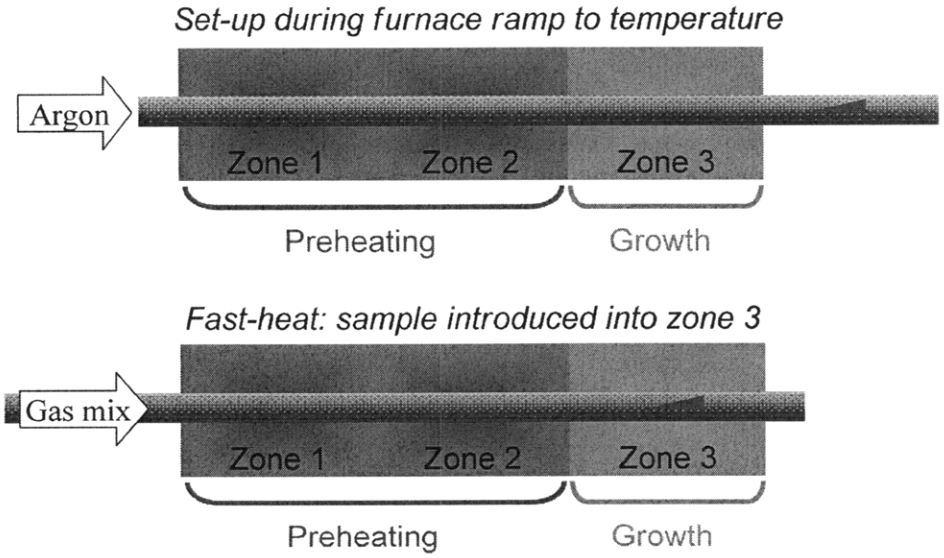

Figure 7. Image and Schematic of Furnace System.
Picture of 3-zone furnace set-up and schematic of fast-heat technique. (Courtesy of Gilbert Nessim)

Experimental Methods

Sample Preparation

The samples used in this study consisted of coupons with metallic square pads with sizes varying from 10 to 100 microns. The metals constituting the catalyst stack were e-beam evaporated using a CHA bell jar evaporator with a 4-pocket Temescal source. The base pressure was between 2.0 10^{-6} Torr and 2.0 10^{-7} Torr. We evaporated 5nm of Ta (as an adhesion layer), 200nm of Cu, 30nm of Ta (underlayer) and 2nm of Fe (catalyst) on silicon without breaking vacuum. Additional samples were constructed with a layer of Pd deposited prior to the Cu layer. A standard lift-off process was used to generate the square pads. The samples were prepared on 2"-square oxidized silicon substrates and were manually cleaved to form approximately 5mm x 5mm pieces that were used during the CNT growth experiments. Samples were cleaned with acetone and isopropyl alcohol prior to CNT growth.

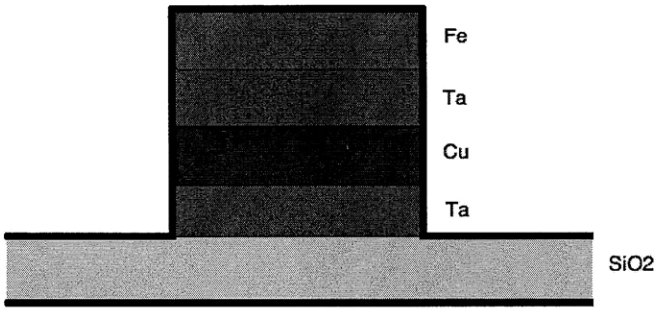

Figure 8. Schematic of cross section of sample.

Growth Conditions

Growth was performed using a three-zone atmospheric-pressure furnace (Lindberg Blue) in a fused-silica tube with an internal diameter of 22 mm. Flows of Ar (99.9995%, Airgas), C_2H_4 (99.5%, Airgas), and H_2 (99.999%, Airgas) were maintained using electronic mass flow controllers (MKS 1179A). The samples were positioned in the quartz tube using a custom-made quartz fixture (Finkenbeiner Glass, Waltham, MA), and faced the flow at an inclination of 20°.

All experiments were performed by using the "fast heat" technique in which the samples were initially positioned in the quartz tube outside the furnace with a fan blowing from below to keep the exposed quartz tube walls at room temperature. An argon flow of 200 standard cubic centimeters per minute (sccm) was maintained while the three zones of the furnace were ramped to the desired temperature. Once the set temperatures were reached, 400 sccm of hydrogen, and 150 sccm of ethylene were introduced and the quartz tube (the sample is sitting on the fixture inside the quartz tube) was shifted, thus positioning the sample in the growth zone and starting the CNT growth process. The growth cycle lasted 15 minutes for each experiment.

The preheating temperatures mentioned for the first two zones (which preheat the gases before they reach the samples) are the ones indicated by the built-in furnace thermocouples. For the third zone, the growth zone where the samples are positioned, in addition to the furnace thermocouple reading, we included the reading from an additional thermocouple (Omega TJ36, accuracy 0.2°C) inserted in the quartz tube (aligned with its axis) and positioned just behind the custom-made quartz fixture containing the samples. This thermocouple was connected to a digital temperature reader (Control Company Traceable Total-Range Thermometer).

Characterization

Scanning Electron Microscopy

The CNTs were examined using high-resolution Scanning Electron Microscopy (SEM - Philips XL30).

Atomic Force Microscopy

Samples that did not include ethylene in the processing were studied using tapping mode AFM (Veeco Multimode SPM).

Purpose of Experiments

The following experiments were completed in an effort to determine the effect oxygen has on the growth of CNTs on conductive substrates, iron catalyst on a tantalum underlayer in particular. Vertically-aligned CNTs (VA-CNTs) are of particular interest as they would be useful in filling vias in semiconductor applications. The process involved initial observations via SEM followed by an optimization of conditions, and concluded with AFM scans to test hypotheses for growth methods.

Results

Initial Observations

Initial growth runs were performed to determine the optimum temperature settings and preferable oxygen content for growth of VA-CNTs. During these runs both iron tantalum (Fe-Ta) and nickel palladium (Ni-Pd) systems were studied. The Fe-Ta samples consisted of two distinctive layer patterns: Fe-Ta-Cu-Pd-Ta-SiO_2 and Fe-Ta-Cu-Ta-SiO_2 referred to as the Conductive and Standard samples respectively. Ni-Pd systems also had two variants, one with a nickel layer with a thickness of 25nm and the other with a larger thickness of 500nm.

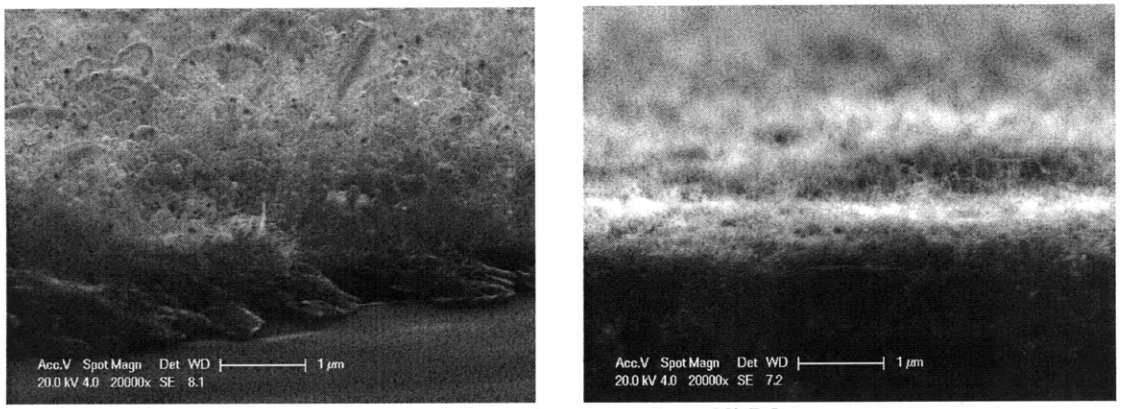

Figure 9. Initial CNT growth on Ni-Pd
SEM images of Ni-Pd 500 nm (left) and 25 nm (right).
Growth conditions – Temperature - 740/740/500, 8 min growth, 398.5Ar/1.5Ar-O_2/800H_2/250C_2H_4

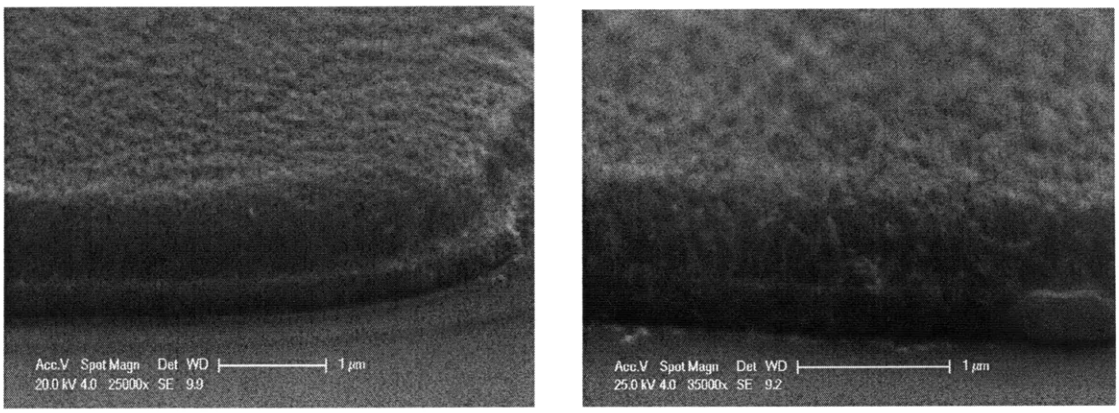

Figure 10. Initial CNT growth on Fe-Ta.
SEM images of Fe-Ta (Standard) in which increased oxygen content led to dense and better-aligned CNT.
Growth conditions (left) – Temperature - 740/740/500, 8 min growth, 397Ar/3Ar-O_2/800H_2/250C_2H_4
Growth conditions (right) – Temperature - 740/740/500, 8 min growth, 399.5Ar/0.5Ar-O_2/800H_2/250C_2H_4

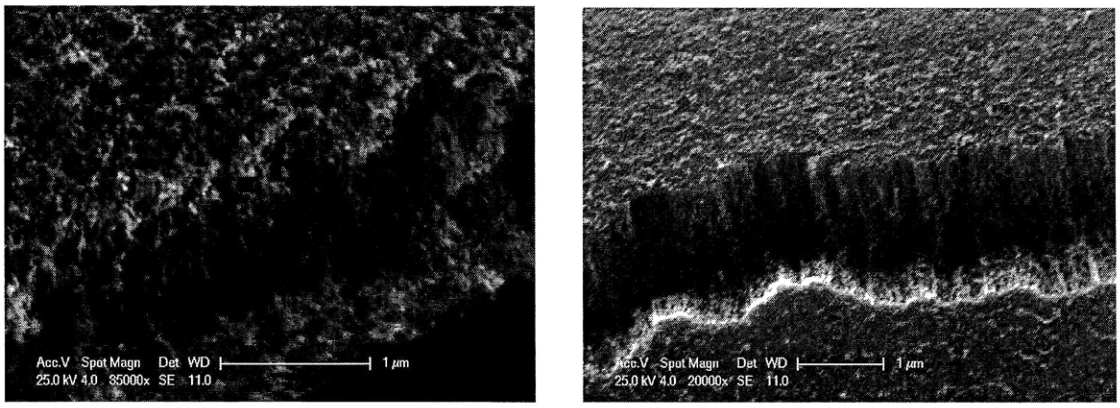

Figure 11. Initial CNT growth on Fe-Ta for Standard and Conductive Substrates.
SEM images of Fe-Ta. Standard (left) and Conductive (right).
Growth conditions – Temperature - 770/770/475, 15 min growth, 399.5Ar/0.5Ar-O_2/800H_2/250C_2H_4

Based on initial observations of the role of O_2, we performed a systematic study of CNT growth dependence on O_2 content in the atmosphere.

Oxygen Series

Each run followed the parameters previously determined to be most optimal with variations in Ar/O_2 levels ranging from 0-30 sccm, with pure Ar balancing the flow rate to remain at a total of 400 sccm.

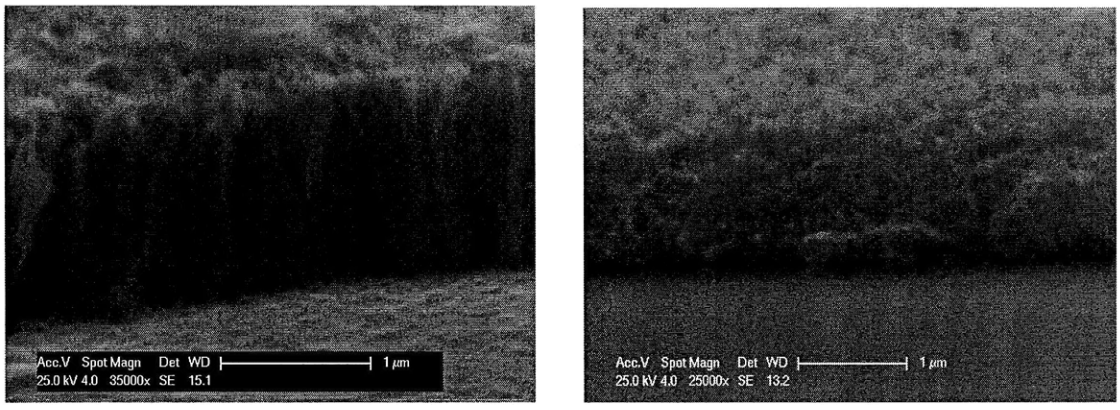

(a) (b)

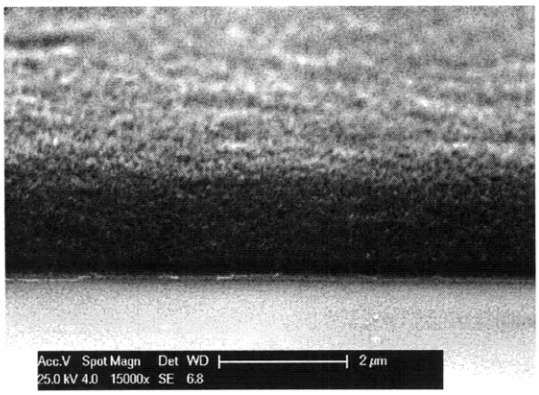

(c)

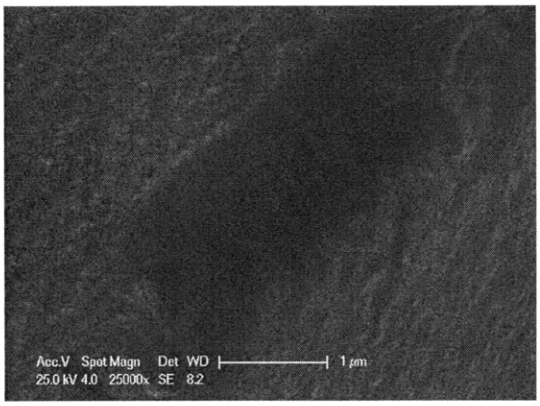

(d)

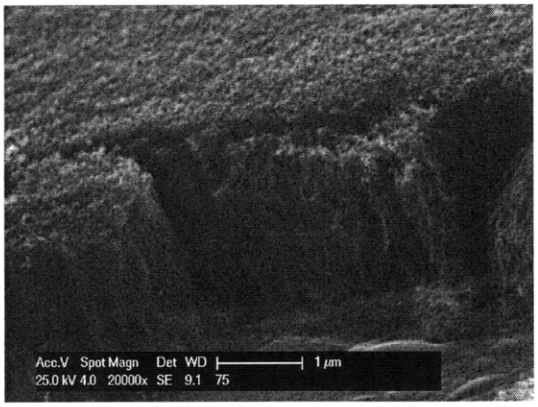

(e)

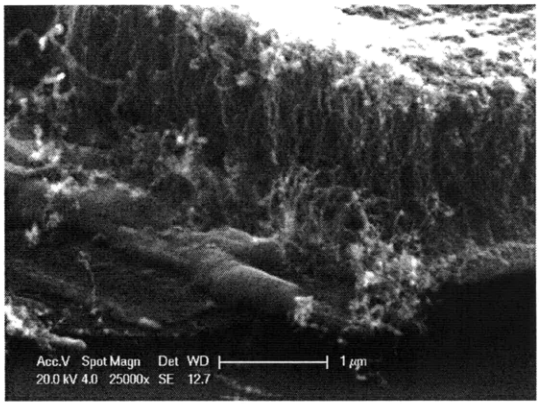

(f)

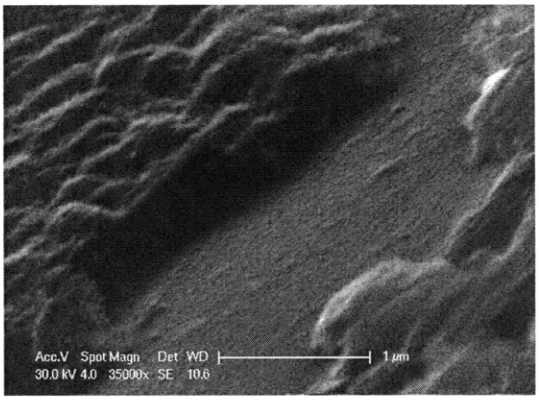

(g)

Figure 12. Resulting Images of oxygen series on Fe-Ta (Standard).
SEM images of Fe-Ta (Standard) including ranges of
(a) 0, (b) 0.1, (c) 0.5, (d) 2, (e) 5, (f) 10, and (g) 30 sccm.

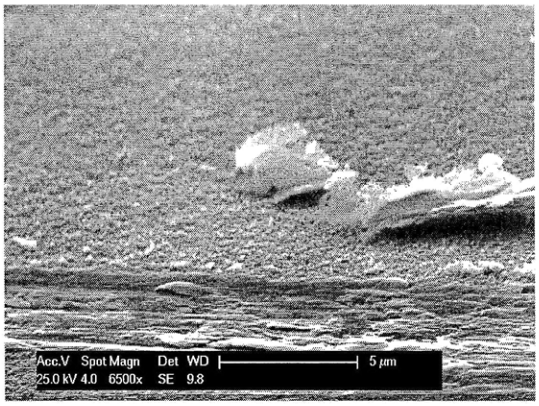
Acc.V Spot Magn Det WD 5 μm
25.0 kV 4.0 6500x SE 9.8

(a)

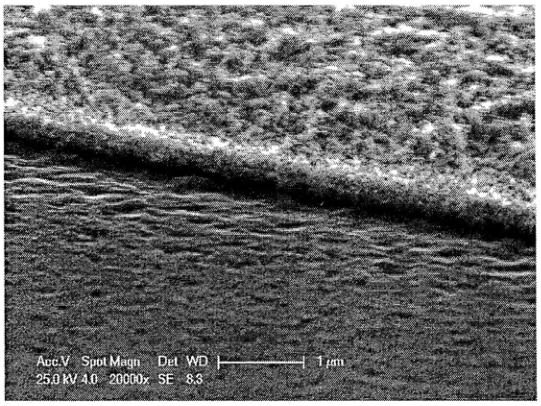
Acc.V Spot Magn Det WD 1 μm
25.0 kV 4.0 20000x SE 8.3

(b)

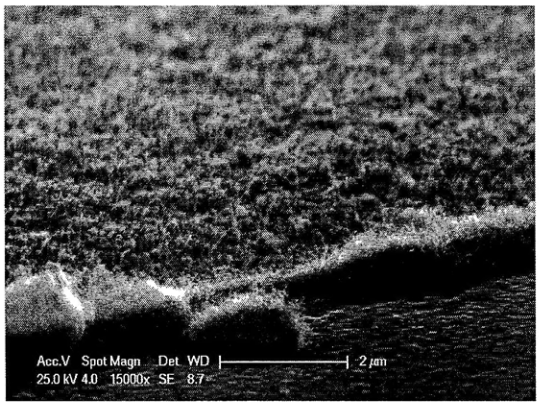
Acc.V Spot Magn Det WD 2 μm
25.0 kV 4.0 15000x SE 8.7

(c)

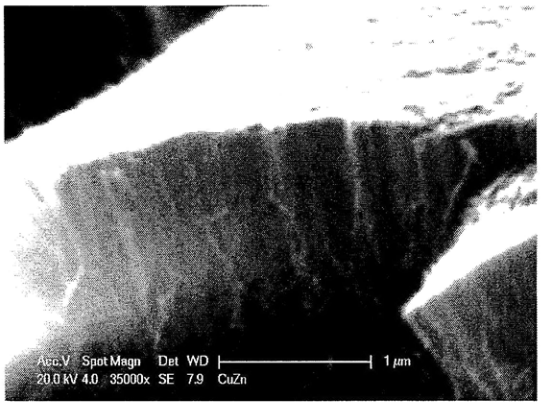
Acc.V Spot Magn Det WD 1 μm
20.0 kV 4.0 35000x SE 7.9 CuZn

(d)

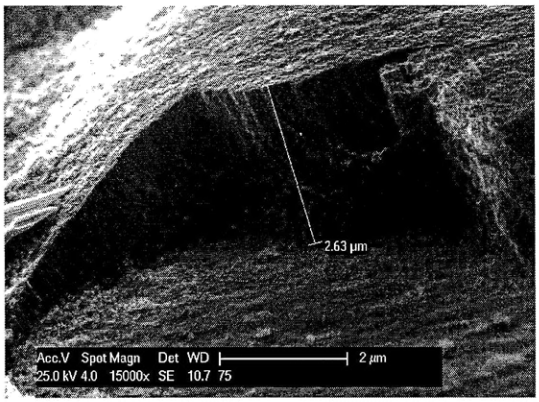
2.63 μm
Acc.V Spot Magn Det WD 2 μm
25.0 kV 4.0 15000x SE 10.7 75

(e)

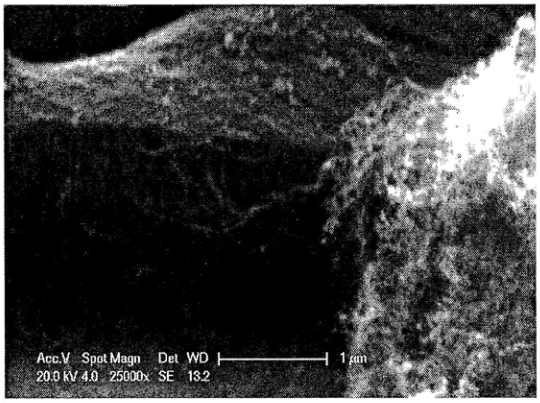
Acc.V Spot Magn Det WD 1 μm
20.0 kV 4.0 25000x SE 13.2

(f)

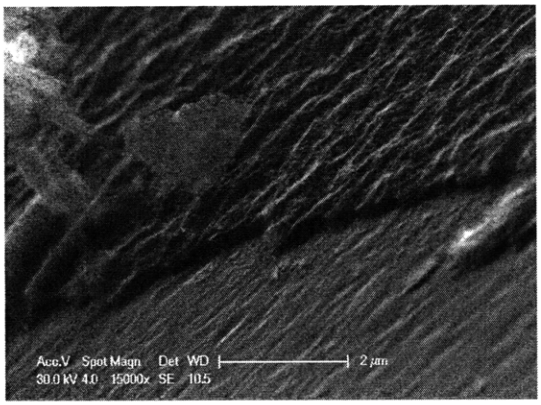

(g)

Figure 13. Resulting Images of oxygen series on Fe-Ta (Conductive).
SEM images of Fe-Ta (Conductive) including ranges of
(a) 0, (b) 0.1, (c) 0.5, (d) 2, (e) 5, (f) 10, and (g) 30 sccm.

When taken relative to each other, there is an obvious trend in the height profiles of each of the samples as a function of oxygen content. This trend is tabulated in the following graph, which shows the relative heights of the CNTs throughout the oxygen series for both standard and conductive samples.

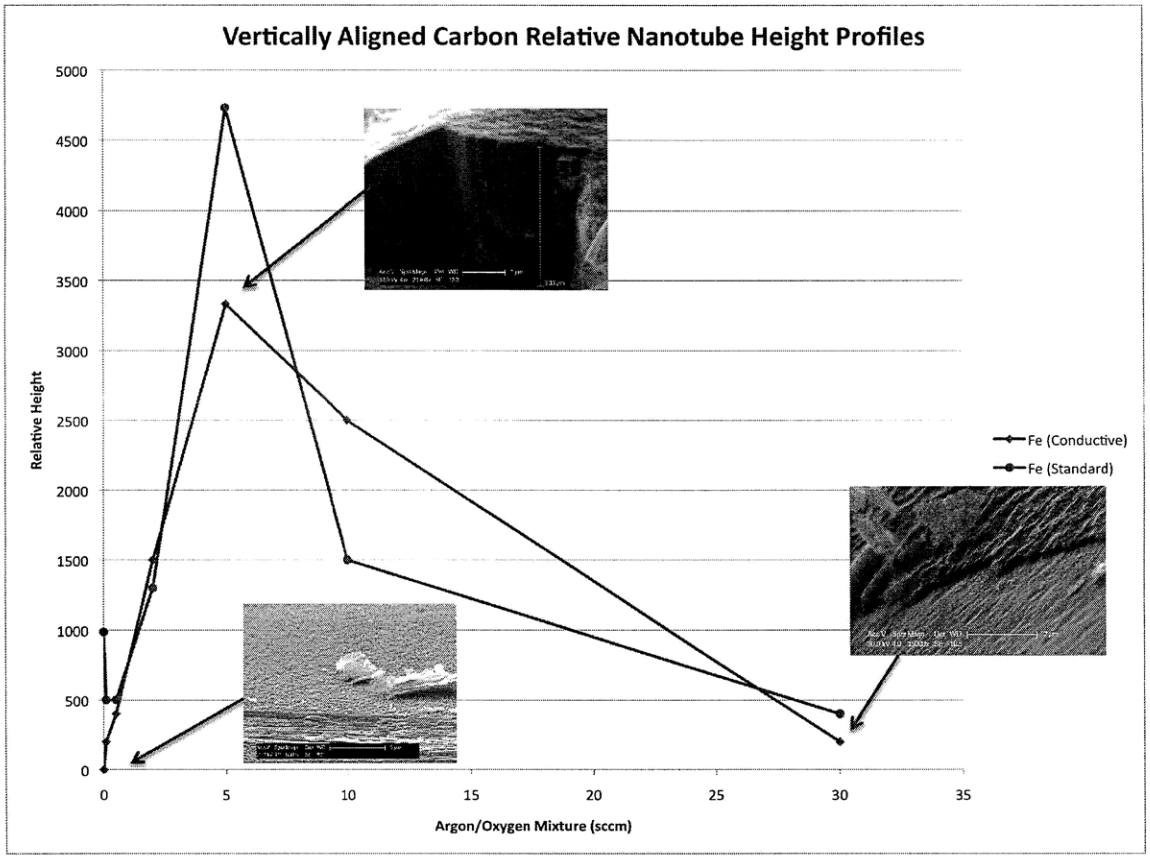

Figure 14. Trends in CNT growth as a function of Ar/O_2 present during growth.
Relative height profile of CNT throughout oxygen series with 5 sccm of Ar/O_2 showing extensive growth when compared to other samples in the series.

From the height profiles the best results stem from the recipe containing 5 sccm of the Ar/O_2 mixture. As this recipe has shown the optimum growth characteristics, it is used in future experiments to test the effects pre-annealing the samples prior to growth will have in different environments.

Pre-Annealing Experiments

Once the relationship between growth height and oxygen levels was determined, the optimal recipe was then used in pre-annealing tests. The samples were placed in the furnace in

either an oxygen-rich or hydrogen-rich environment for 4 minutes. After the 4 minutes transpired, the other gasses were flown in for an additional 20 minutes of growth.

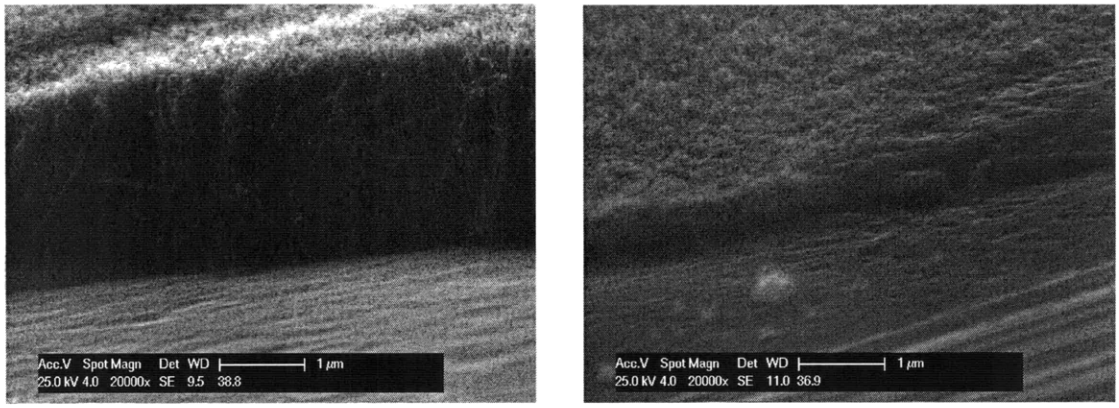

Figure 15. Pre-anneal of Conductive Substrates.
SEM images of Fe-Ta (Conductive) pre-annealed in an oxygen-rich environment (left) and a hydrogen-rich environment (right).

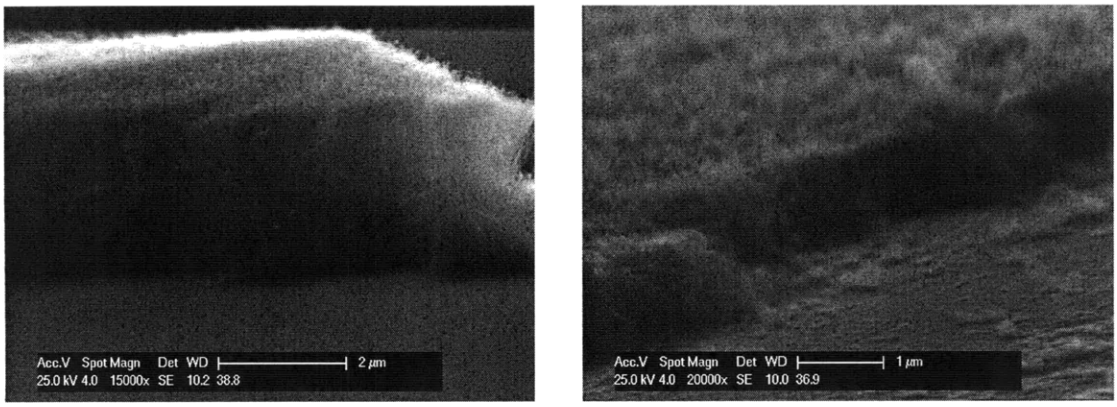

Figure 16. Pre-anneal of Standard Substrates.
SEM images of Fe-Ta (Standard) pre-annealed in an oxygen-rich environment (left) and a hydrogen-rich environment (right).

AFM Measurements

In an effort to understand potential growth mechanisms for CNTs and how the oxygen or hydrogen rich environments affect the catalysis, AFM scans were performed. The morphology of the sample during processing is important in determining the possible growth characteristics.

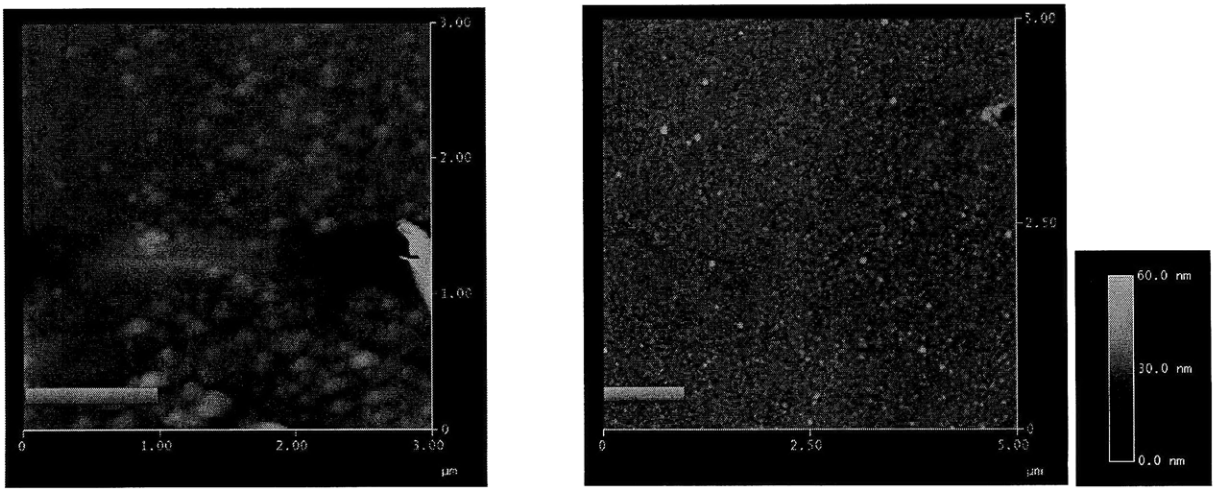

Figure 17. Morphology scans of Fe-Ta prior to processing.
Standard (left) and Conductive (right). Scale bars are 1 μm. Imaged by Hsu-Yi Lee.

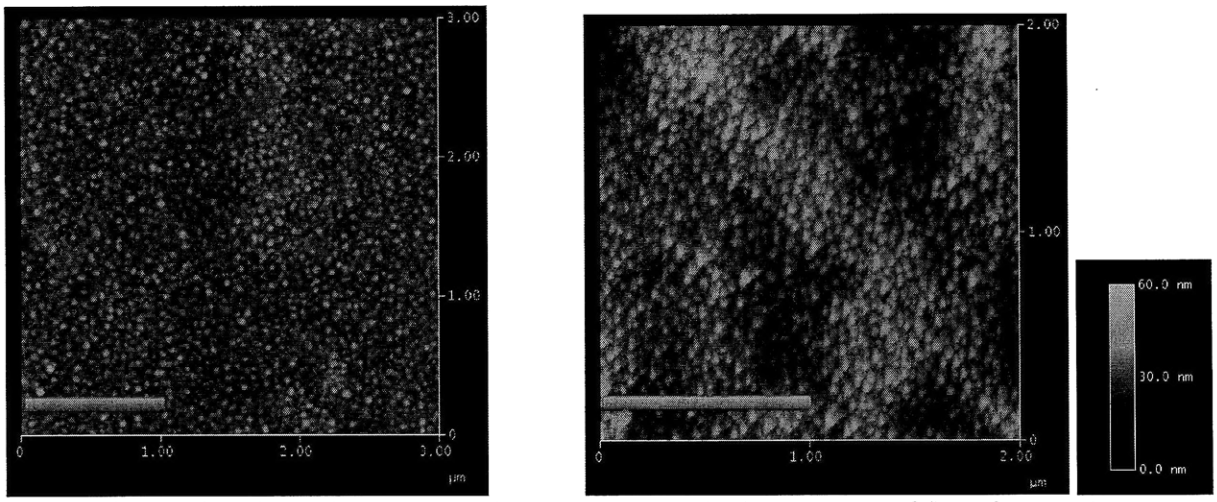

Figure 18. Morphology scans of Fe-Ta after processing in an oxygen-rich environment.
Standard (left) and Conductive (right). Scale bars are 1 μm. Imaged by Hsu-Yi Lee.

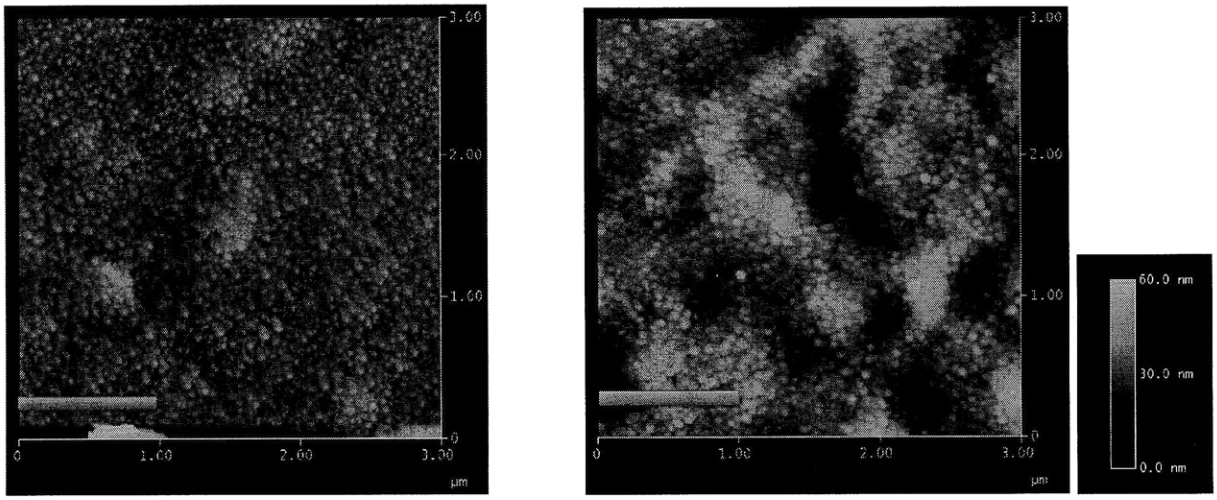

Figure 19. Morphology scans of Fe-Ta after processing in an hydrogen-rich environment.
Standard (left) and Conductive (right). Scale bars are 1 μm. Imaged by Hsu-Yi Lee.

Interpretation

The oxygen series indicates that the height and packing density of CNTs have a strong dependence on the oxygen content. The low-oxygen images show very limited growth, with no appreciable CNT formations. This indicates that some oxygen is necessary for consistent growth. With increasing oxygen content, the growth does not seem to change until reaching 2 sccm of the Ar/O_2 mixture, at which large formations are visible. After reaching 10 sccm of Ar/O_2 the formations appear to be less well defined, and 30 sccm shows very little growth, similar to growth heights of 0-0.5 sccm. [Figure 12 and Figure 13]

The pre-annealing tests demonstrate the effect oxygen and hydrogen have on the development of CNTs when the sample is exposed to the environment prior to growth. The oxygen-rich environment shows growth nominally larger than that of the reference. The hydrogen-rich environment had far smaller growth, comparable to previous experiments that had much lower oxygen content than the optimum percentage. The predicted effects of the oxygen and hydrogen are to reduce and promote coarsening respectively. Coarsening is suspected as a mechanism that affects the growth patterns of CNTs. As catalyst particles congregate they form areas of high and low concentrations of particles, leading to non-uniform growth of CNTs. In addition, a uniform distribution of catalysts is suspected to promote steric effects forcing vertical growth of CNTs.

In order to confirm the hypothesis of the effect of pre-annealing on the surface morphology, the surface of samples were scanned using AFM. The AFM scans show supporting evidence of the hypothesis with catalyst apparently coarsening in the hydrogen rich as shown in Figure 19. Coarsening is thought to provide larger catalyst particles which lead to tubes with larger diameters, but with less dense packing. The images show what appears to be movement of

catalyst particles, indicated with the lighter coloring, towards regions indicative of potential coarsening.

In addition to these results other work has shown a positive effect of oxygen on growth characteristics. (Futaba, Hata, & Iijima, 2006) In this work, the authors used 150 ppm of H_2O as a source of oxygen to enhance growth. Using the recipe demonstrating optimal growth characteristics, and assumption of complete reaction with all O_2 present within the Ar/O_2 mixture at the reaction temperatures (Bielański & Haber, 1991), the H_2O present in our experiments is estimated to be ~70 ppm. This is within an order of magnitude of the recipes used by Futaba et al. and provides similar results. Controlling the environment of these experiments does not require the use of expensive and constrictive requirements of humidity control as was seen in Futaba et al., but instead requires only gas canisters of a specific purity and a mass flow controller.

Conclusion

CNT growth is largely affected by the presence of oxygen during growth, both prior to and during the growth step. There is an optimum presence at which growth is greatly enhanced, but outside of this range, oxygen appears to have a negative effect on the growth characteristics.

Also, additional oxygen prior to growth appears to slightly enhance the growth of VA-CNTs. A possible explanation of this behavior is due to reduction of coarsening in the oxygen-rich environment. The lack of coarsening provides a more favorable morphology for the growth of VA-CNT, as catalyst particles are smaller and closer in proximity to each other.

Future Work

There are a number of ways to test inferences made here. Due to a limited amount of time, most experiments were not repeated, and should be repeatability.

Performing further experiments in the oxygen series would also be beneficial. There is a large gap in the height profile of growth between 0.5 sccm and 2 sccm of Ar/O_2, which does not indicate the precise amount of oxygen needed for long CNTs.

Electrical characterization of the CNTs would be an additional test that would be useful in determining the electrical conductivity of the CNTs grown in the oxygen-rich environment.

Transmission Electron Microscopy (TEM) would be useful in determining the crystallinity and confirming the growth of nanotubes as opposed to other possible carbon structures. TEM would also serve a method of directly observing the CNT diameter and associated catalyst particles. This would allow direct observations of any correlations between CNT diameter and catalyst size.

Acknowledgements

I would like to thank my advisor, Professor Carl V. Thompson for his support of this project. I would also like to thank Gilbert D. Nessim for his help and guidance throughout the entire project. Also, thanks to Hsu-Yi Lee for her assitance with performing the AFM scans.

Many thanks to Christina Prudent for all of her patience and support.

Bibliography

Bielański, A., & Haber, J. (1991). *Oxygen in Catalysis.* CRC Press.

Dresselhaus, M. S., Dresselhaus, G., & Avouris, P. (2001). *Carbon nanotubes: synthesis, structure, properties, and applications.* Springer.

Futaba, D. N., Hata, K., & Iijima, S. (2006). 84% Catalyst Activity of Water-Assisted Growth of Single Walled Carbon Nanotube Forest Characterization by a Statistical and Macroscopic Approach. *J. Phys. Chem. B* , 8035-8038.

Hata, K., Futaba, D. N., Mizuno, K., Namai, T., Yumura, M., & Iijima, S. (2004). Water-Assisted Highly Efficient Synthesis of Impurity-Free Single-Walled Carbon Nanotubes. *Science , 306*, 1362-1364.

Odom, T. W., Huang, J.-L., Kim, P., & Lieber, C. M. (2000). Structure and Electronic Properties of Carbon Nanotubes. *J. Phys. Chem.* , 2794-2809.

Seita, M. (2007). *Low Temperature Growth of Crystalline, Vertically Aligned Carbon Nanotubes on Conductive Substrates for Interconnect Applications.*